

Molecular Modeling of Quinoline-Based Compounds as Potential Dual Inhibitors of Reverse Transcriptase and Integrase of HIV

Alberto Cabrera^{1*}, Leonor Huerta Hernández², Daniel Chávez³, José L. Medina-Franco^{1*}

¹Departamento de Farmacia, Facultad de Química, Universidad Nacional Autónoma de México, México City, México

²Instituto de Investigaciones Biomédicas, Universidad Nacional Autónoma de México, México City, México

³Centro de Graduados e Investigación en Química del Instituto Tecnológico de Tijuana, Tijuana, México

Email: *jaques_yves@hotmail.com, *jose.medina.franco@gmail.com

How to cite this paper: Cabrera, A., Hernández, L.H., Chávez, D. and Medina-Franco, J.L. (2018) Molecular Modeling of Quinoline-Based Compounds as Potential Dual Inhibitors of Reverse Transcriptase and Integrase of HIV. *Computational Molecular Bioscience*, 8, 122-148.

<https://doi.org/10.4236/cmb.2018.83007>

Received: July 16, 2018

Accepted: August 4, 2018

Published: August 7, 2018

Copyright © 2018 by authors and Scientific Research Publishing Inc. This work is licensed under the Creative Commons Attribution International License (CC BY 4.0).

<http://creativecommons.org/licenses/by/4.0/>



Open Access

Abstract

As follow-up of our past publication [1], we propose that quinolones (as part of the pyridinone family) are capable to increase the number of interactions with HIV reverse transcriptase (RT) or integrase (IN) by adding a halogen in position C-8 of aromatic portion of the quinolones. This addition could help with the activity of dual inhibitors of RT and IN. In this work, we add a chlorine atom with the rationale to identify in the docking simulations a halogen interaction with the oxygen in the near aminoacids in the binding pockets of RT and IN enzymes. Our docking studies started with RT and 320 structures. Later, we took 73 structures with good results in docking with RT. The structures that we choose contain ester or acids groups in C-3 due the structural similarity with groups in charge to interact with the Mg⁺⁺ ions in Elvitegravir. In conclusion, we obtained 14 structures that could occupy the allosteric pocket of RT and could inhibit the catalytic activity of IN, for this reason could be dual inhibitors. A major perspective of this work is the synthesis and testing of the potential dual inhibitors designed.

Keywords

Reverse Transcriptase, Integrase, Quinolone, Dual Inhibitor, Docking

1. Introduction

In our research group we were working with pyridinone derivates as antiretroviral against HIV-1 [1] [2]. This kind of compounds belongs to a family of non-nucleoside reverse transcriptase inhibitors (NNRTI) [3]. In our last publica-

tion we could observe that quinolones have big possibilities to be inhibitors of RT and IN [1]. The structures of pyridinone derivates have the possibility to interact with conserved aminoacids in RT to inhibit the activity of the enzyme [4] [5]. Also, the substituents in the pyridinone derivates could interact with Mg^{++} ions located in a small space between DNA and IN in the nucleus of the cell. This is to avoid that the enzyme IN blocks the action of DNA as proposed by Wang *et al.* [6]. The quinolone ring has an aromatic portion facilitating the making of analogues or adding substituents that could contribute to the activity of the compounds. Based on this rationale, here we designed compounds that have in common a chlorine substituent in C-8 of the quinolones and have the basic structure of the pharmacophore published by Freeman *et al.* [7]. The new structures were designed according with the matrix in **Figure 1**. Some structures have ester and acid substituent that could give to the compounds the possibility to be dual inhibitors [6] [8]. Some structures contain a hydroxyl substituent in N-1 in a similar way as is published by Wang *et al.* [5]. As we can see, the structures show one to three halogens in total but two of the halogens in some of the structures remain in positions C-6 and C-8 of the aromatic ring. It's possible that the chlorine in C-8 position could contribute in the activity of the molecule of quinolone as RT or IN inhibitor due a halogen bond with other aminoacids [9].

Actually, multi-halogenated compounds belong to the HAART therapy against HIV infection because they are bioactive. As an example of halogenated drugs

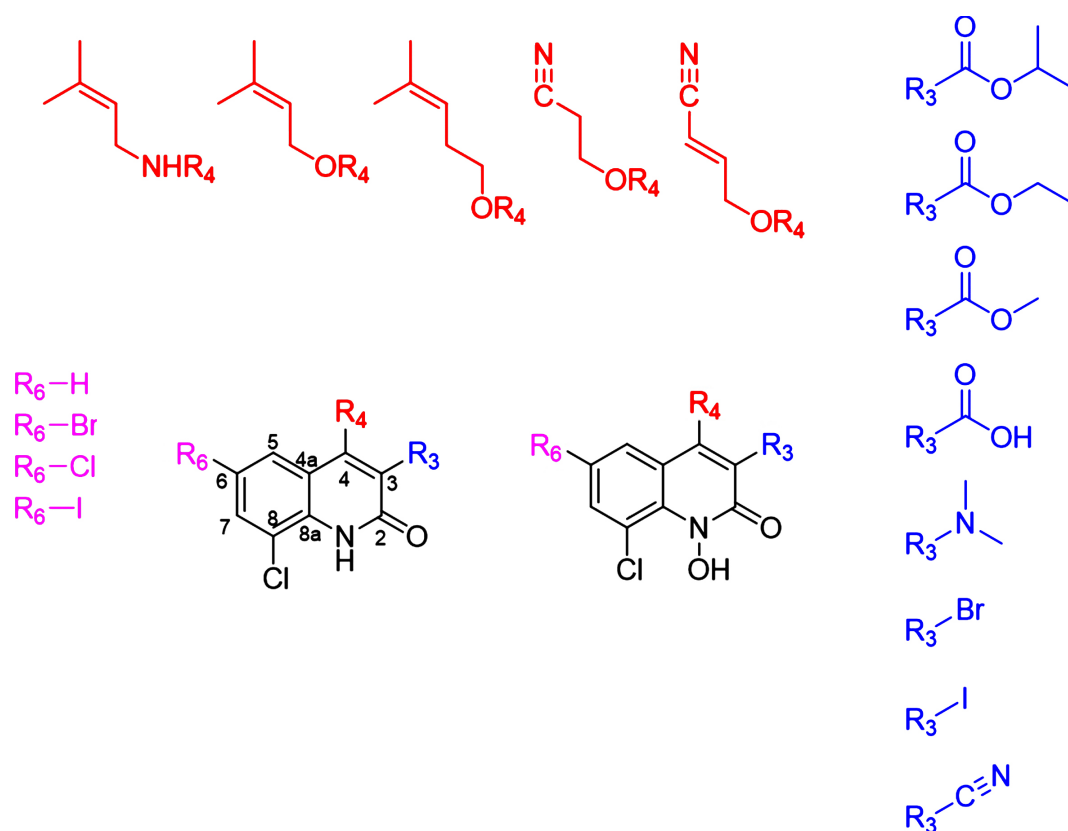


Figure 1. Chemical structures of the quinolone derivatives considered in this work.

against HIV **Figure 2** shows six drugs. These drugs have been authorized by the Food and Drug Administration (FDA) of the USA. Doravirine is in Phase III of its development. **Figure 2** shows halogenated and multihalogenated compounds against RT and IN. The RT inhibitors halogenated are Efavirenz, Doravirine and Etravirine; and the IN inhibitors are Raltegravir, Elvitegravir and Dolutegravir [10] [11].

The objective of this work is to propose new compounds with dual activity against RT and IN which contains halogens that contribute to the activity against HIV-1 and that could reduce the quantity of drugs to be taken orally. The infected persons have to take several pills in a treatment called HAART that have secondary effects. If the quantity of drugs is reduced, the secondary effects will be reduced and will be a benefit to the treated patients [12].

2. Methods

Based on the scheme of structures analyzed in our previous publication [1] we propose 320 chemical structures that are synthetically accessible. The goal is to maintain the main structural characteristics of the hybrid pyridinone-UC781 molecule [4] but using the quinolone scaffold according to the matrix of substituent in **Figure 2**. In general, the design was constituted by a polar group at C-3 and an unsaturated aliphatic chain in C-4 of the scaffold of quinolone. The scaffold of quinolone in all the schemes has a chlorine in C-8 with the goal of increasing the interactions with the binding sites of RT and IN and, overall, improving its activity as potential dual inhibitors. The design of some quinolones

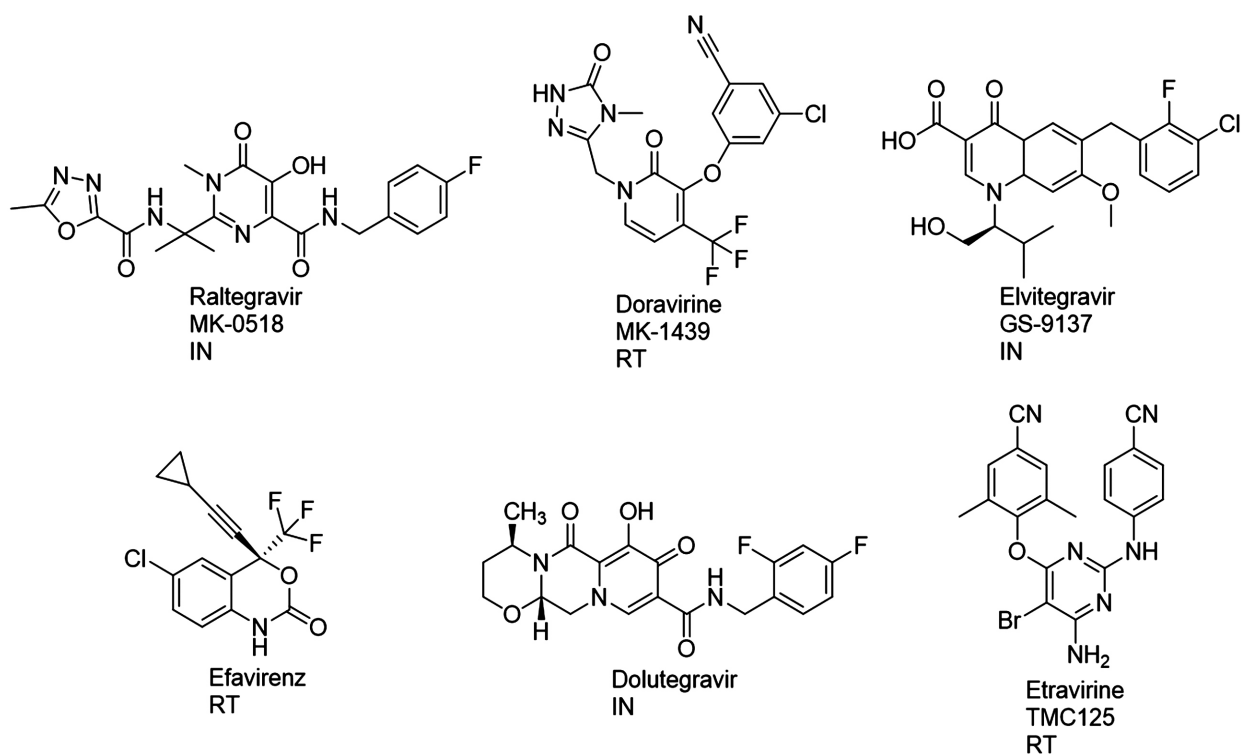


Figure 2. Drugs halogenated and multihalogenated inhibitors of RT and IN of HIV.

was inspired in the compounds developed by Wang *et al.* [6] because contain an N-OH substitution.

For the docking studies described below, the crystallographic structures of the biomolecular targets were retrieved from the Protein Data Bank (PDB) (<http://www.rcsb.org>) [13]. **Table 1** summarizes the information of the two structures of RT [14] and one for IN [15] used in this work. The **Table 1** includes the information of the co-crystallized ligand in each structure. All computational studies were conducted with Molecular Operating Environment (MOE) software, version 2014 [16] to make the results comparable with the previous published study [1].

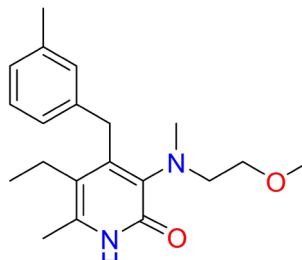
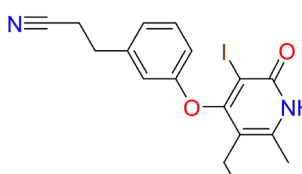
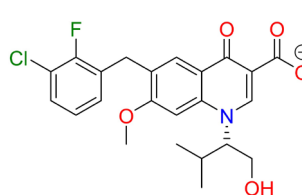
2.1. Structure Preparation

This study is a continuation of our previous results published [1]. The same structures were used. The full details of the preparation of the structures are published in Cabrera *et al.* [1].

2.2. Validation of Docking Protocol

Similar to the previous work [1] before docking of the halogenated structures of the **Figure 1**, the docking protocol was validated by re-docking of the co-crystal ligands in their corresponding crystallographic structure. As reference, **Table 1** shows the ligands and their respective enzymes used in validation. For this validation were considered semi-flexible the three co-crystal ligands (R165481, R157208 and GS9137) and was done with the MMFF94x force field with the

Table 1. Summary of the crystallographic structures of RT and IN used in this work.

PDB ID	Resolution (Å)	ID ligand	Co-crystallized ligand
2BAN (RT)	2.95	R157208	
2B5J (RT)	2.90	R165481 Note: the tautomeric conformation is taken	
3L2U (IN)	3.15	GS9137 (Elvitegravir)	

default settings of MOE [16] (e.g., 500 iterations in total with 30 consecutive attempts to select the best result). The binding pocket was defined as the set of amino acids within of 4.5 Å of the co-crystal ligand.

2.3. 3D flexible Alignment of Pyridinone Structures

The flexible alignment of the new quinolones structures was performed to explore if these new structures could adopt similar conformation as the co-crystallized pyridinone analogues. Similar to our previous work, we selected a sample of 10% (32 structures) and each was aligned flexibly to the co-crystal coordinates of R157208 and R165481. For this study, the structure of the co-crystal compound was kept rigid. The docking was conducted with MOE maintaining the default settings (500 iterations in total with 30 consecutive attempts to find the best result) with the MMFF94x force field.

2.4. Docking

2.4.1. Docking with RT

For this study, 320 quinolone structures were docked with the crystallographic structures PDB ID: 2BAN and 2B5J [13] and the same settings of the validation were maintained. As result of the docking with the two crystallographic structures, 73 structures were selected to further analysis with IN. In the process of analysis, the protein ligand interaction fingerprints (PLIFs) were important to select the 73 structures. PLIFs were generated with MOE ligand.

2.4.2. Docking with IN

For 73 structures were selected based on the similarity with the functional groups and binding poses with known dual inhibitors of RT and IN. The 73 structures were docked with the crystallographic structure PDB ID: 3L2U with the same parameters used in the docking of the crystal ligand (Elvitegravir, GS9137) [15].

2.5. Calculation of Drug-Like Properties

In order to explore the potential oral bioavailability of the structures proposed, we calculated the pharmaceutical properties molecular weight (MW), the partition coefficient octanol/water (Log P) as a measure of lipophilicity, topological polar surface area (TPSA), number of hydrogen bond donors (HBD), number of hydrogen bond acceptors (HBA), and number of rotatable bonds (RB) [17] [18].

3. Results and Discussion

3.1. Alignment of Crystallographic Structures of RT

The coordinates obtained in our previous work [1] of the structures aligned and superposed were used to run the docking using 320 structures of pyridinone derivatives. The structures selected for this study were PDB ID: 2BAN and 2B5J [13].

3.2. Validation of the Docking Protocol with RT

Before docking the newly structures proposed in this work (**Figure 1**), the

docking protocol was validated as described in the Methods section. The root-mean square deviation (RMSD) values between the co-crystal and predicted positions were low: the RMSD values were 0.8222 and 0.7393 for 2BAN and 2B5J, respectively. The relative docking scores obtained were -9.1224 and -8.6151 for 2BAN and 2B5J, respectively. These results indicate that the settings used in the docking are correct to reproduce the binding modes shown in the crystal structure.

3.3. Alignment with Co-Crystallized Pyridinone Derivatives

A sample of 10% of the data (32 structures) was taken of the 320 structures in a scheme of stratified random sampling. The structures were aligned flexibly with the position of crystallographic structures of R157208 and R165481 (**Table 1**). In the analysis of the results, the best values were obtained for the structures aligned with R165481. The results were not so different to those obtained in the previous work [1]. In this study, the values of alignment of the new structures with R157208 were less negative than the values of the alignment of the same structures but with R165481. The 32 structures with R157208 had an average of alignment energy of -80.05 Kcal/mol with a standard deviation of ± 9.58 Kcal/mol. The average of alignment energy for R165481 was -83.40 Kcal/mol and standard deviation of ± 11.14 Kcal/mol (Table of 3D alignment results in supplementary material as **Table S1**). As an example of the alignment, **Figure 3** shows the 3D alignment of structures **180** and **270** with R157208 and R165481, respectively. The results of the alignments of structures **180** and **270** are close to the average values and are possible to observe the good overlap with reference structures.

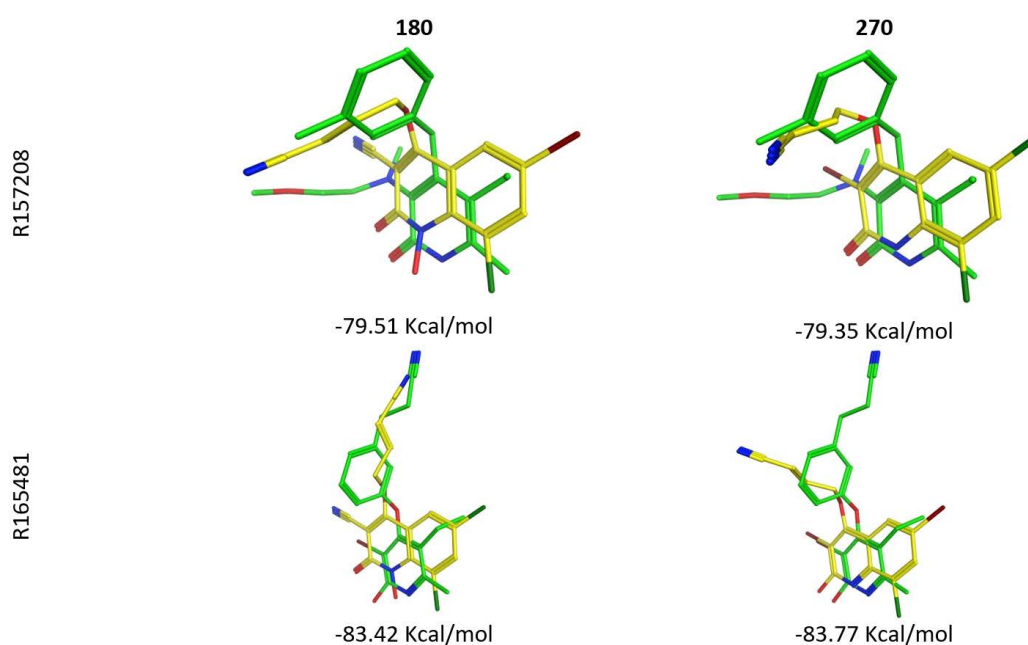


Figure 3. Alignment of the structures **180** and **270** with R157208 and R165481.

3.4. Binding Modes with RT, PDB ID: 2BAN

After the docking assay performed with MOE for 320 new molecules using PDB ID: 2BAN, we select 72 structures maintaining interaction with important aminoacids for this investigation. The contacts of interest observed were between the substituent in C-4 of each molecule with Tyr188 and the conserved aminoacids Trp229; and the interaction of substituent in C-3 with conserved aminoacid Pro236 due to a 180° rotation of the molecule but always maintaining the characteristic interaction of pyridinones and other non-nucleoside RT inhibitors [19] [20] [21] between hydrogen in N-1 and the oxygen of Lys101 (**Figure 4**). Pro236 was the aminoacid with most contacts with the ligand. Another common interaction observed with the docked molecules was with the chlorine atom in C-8 and the oxygen of the carbonyl group in Pro236. The distances shown for the structures that have halogen bond are between 2.9 and 3.5 Å.

Also, is important to indicate that as result of docking we could identify some structures with double interaction with aminoacids of interest because at the same time show the possibility to have contacts with Pro236 and Tyr188 (structures **152** and **181**); and contacts with Pro236 and Trp229 observed in the structures **123** and **158** (**Figure 5**). The structures mentioned have good results of score as we can see in the **Table 2**.

In general, **Table 2** highlights seven structures with the best results and 10 structures with less favorable results. This distinction is based on the relation of average and standard deviation in the docking assay with PDB ID: 2BAN.

Structures with multiple interactions with aminoacids of interest have better possibilities as inhibitors according with the docking with 2BAN.

3.5. Binding Modes with RT, PDB ID: 2B5J

The results of docking of 320 structures with PDB ID: 2B5J helped us to identify

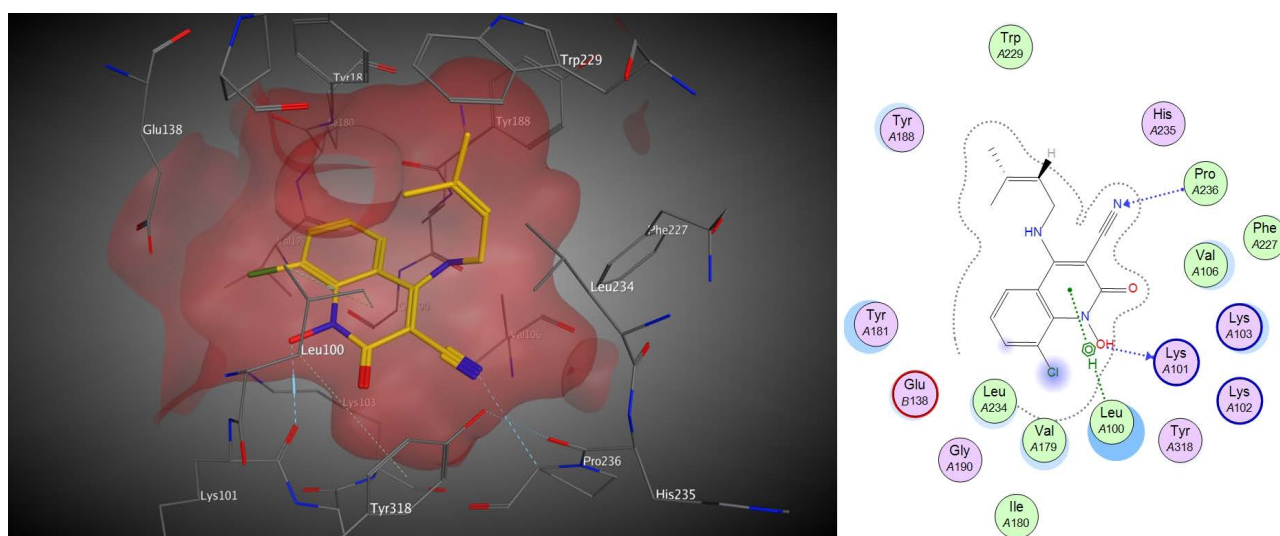


Figure 4. Docking model of molecule **146** with the structure of RT PDB ID: 2BAN. The model shows interaction characteristic between NOH and the oxygen of the carbonyl group of Lys101; and interaction between substituent in C-3 and Pro236.

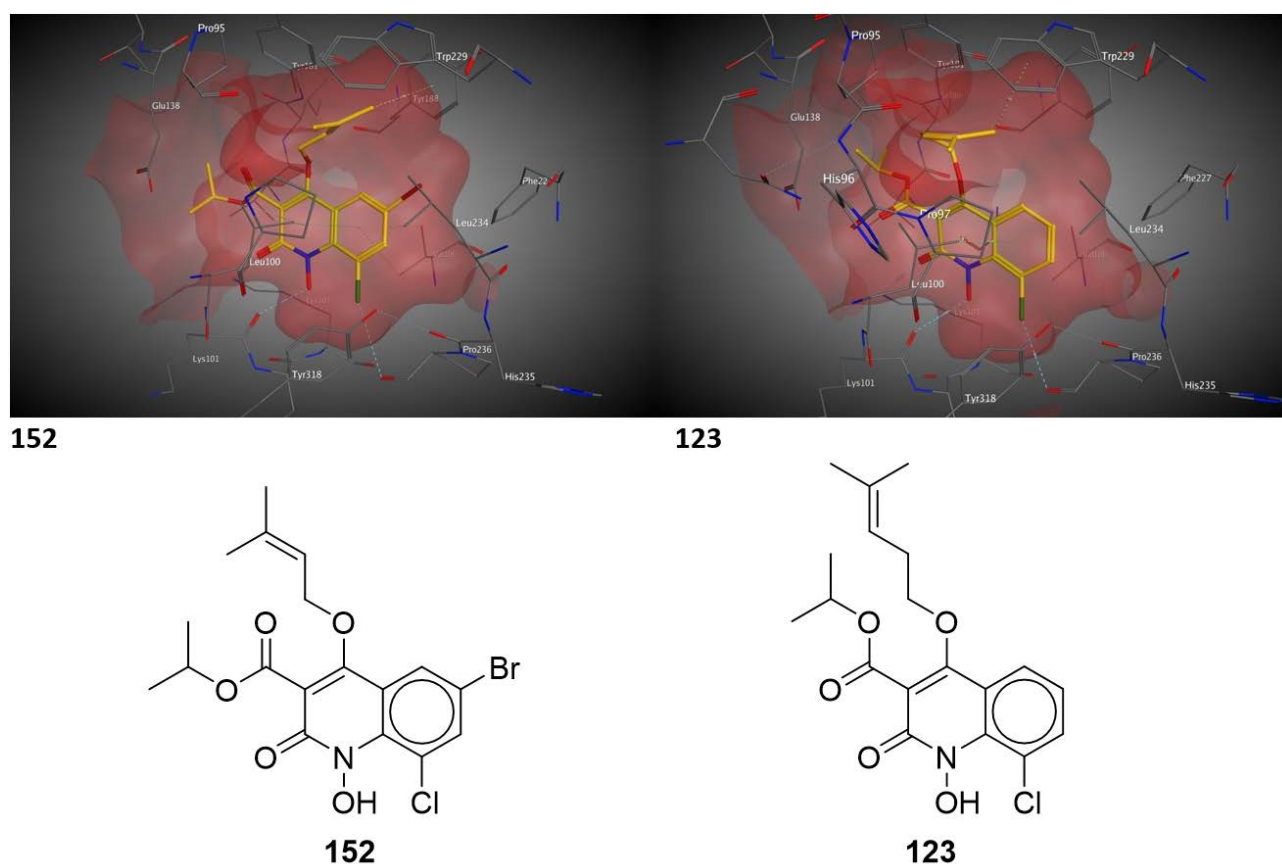


Figure 5. Docking model of structures **152** and **123** showing double interaction with aminoacids in the structure of RT PDB ID: 2BAN. There are contacts with Pro236 and Tyr188 for Structure **152**; and contacts Pro236 and Trp229 for structure **123**.

64 structures with contact with aminoacids of interest as Trp229, Pro236, Tyr181 and Tyr188. The average of score as result of the docking was -7.0418 with a standard deviation of 0.897 in this study. Taking in count the average and the standard deviation, there are 10 outstanding molecules and seven molecules with lower priority (**Table 3**). In general, the most common contact of the ligands is with Trp229.

Docking with the structure PDB ID: 2B5J revealed that compounds **7** and **33** have the possibility to interact with two aminoacids simultaneously with the substituent in C-4 that can confer to the ligands maintain activity against RT. **Figure 6** shows that the substituent in C-4 of compound **7** interacts with Trp229 and Tyr188 at same time while a related substituent at the equivalent position of compound **33** interacts with Tyr181 and Tyr 188.

Another interesting interaction that we observed in docking with quinolones 266 and 270 was a halogen interaction between Iodine and Pro236 as is shown in **Figure 7** for quinolone **270**. The conformation adopted by the ligand enables to contact with Lys101 that is the characteristic interaction of pyridinone.

In the docking performed with PDB ID: 2B5J we could observe less halogen interactions than the docking with PDB ID: 2BAN. The contacts with chlorine in position C-8 are with Lys103. This kind of contact helps to fix the quinolone to

Table 2. Docking results with RT PDB ID: 2BAN. Aminoacid Pro236 without indication of halogen interaction means that the interaction is between substituent in C-3 with Pro236.

# OF STRUCTURE	SCORES	INTERACTIONS	Halogen in C-8 (interaction)
2	-6.479	Tyr188	
3	-6.783	Trp229	
18	-7.452	Tyr188	
26	-7.177	Pro236	
41	-6.919	Trp229	
42	-6.990	Tyr188	
47	-6.829	Trp229	
48	-6.826	Trp229	
58	-7.128	Tyr188	
68	-8.456	Trp229	
72	-7.330	Tyr188	
82	-6.376	Tyr188	
83	-6.870	Trp229	
88	-7.199	Tyr188	
91	-7.619	Tyr188	
92	-6.139	Tyr188	
96	-7.570	Tyr188	
97	-7.624	Tyr188	
99	-7.000	Tyr188	
101	-7.712	Tyr188	
102	-7.918	Tyr188	
104	-5.847	Pro236	Cl-Pro236
107	-7.074	Tyr188	
108	-6.691	Tyr188	
118	-6.832	Trp229	
122	-7.624	Tyr188	
123	-7.175	Pro236, Trp229	Cl-Pro236
128	-6.959	Trp229	
133	-7.206	Trp229	
134	-7.389	Pro236	Cl-Pro236
138	-5.878	Trp229	
145	-6.753	Pro236	Cl-Pro236
146	-7.673	Pro236	
147	-7.355	Pro236	
148	-6.299	Tyr188	

Continued

151	-7.517	Pro236	Cl-Pro236
152	-7.827	Pro236, Tyr188	Cl-Pro236
153	-6.938	Pro236	Cl-Pro236
158	-6.617	Pro236, Trp229	Cl-Pro236
161	-7.501	Pro236, Tyr188	Cl-Pro236
167	-5.387	Tyr188	
169	-6.688	Pro236	Cl-Pro236
170	-6.265	Pro236	Cl-Pro236
178	-4.414	Pro236	Cl-Pro236
181	-7.821	Pro236, Tyr188	Cl-Pro236
182	-8.168	Tyr188	
184	-7.015	Pro236	Cl-Pro236
186	-6.999	Pro236	Cl-Pro236
187	-7.315	Pro236	Cl-Pro236
191	-6.400	Tyr188	
192	-7.287	Pro236	Cl-Pro236
193	-6.334	Trp229	
196	-7.542	Pro236, Tyr188	Cl-Pro236
197	-7.623	Pro236, Tyr188	Cl-Pro236
200	-7.296	Pro236	Cl-Pro236
202	-7.401	Pro236, Tyr188	Cl-Pro236
203	-6.739	Pro236	Cl-Pro236
206	-6.478	Pro236	Cl-Pro236
212	-5.214	Pro236	Cl-Pro236
213	-4.406	Pro236, Tyr188, Trp229	Cl-Pro236
228	-6.818	Tyr188	
253	-7.483	Trp229	
268	-6.996	Tyr188	
276	-7.190	Tyr188	
281	-6.829	Pro236	Cl-Pro236
287	-6.219	Trp229	
292	-6.241	Pro236	Cl-Pro236
295	-6.051	Pro236	Cl-Pro236
308	-4.996	Trp229	
310	-6.887	Pro236	Cl-Pro236
312	-6.015	Tyr188	
316	-5.927	Pro236	Cl-Pro236
Average	-6.861		
Std. Dev.	0.784		

Table 3. Docking results with RT PDB ID: 2B5J.

# OF STRUCTURE	SCORES	INTERACTIONS	Halogen In C-8 (interaction)
1	-7.163	Trp229	
2	-7.085	Trp229	
7	-7.774	Tyr229, Tyr188	
13	-8.080	Trp229	
16	-7.039	Pro236	
20	-6.898	Pro236	
23	-8.864	Trp229	
28	-6.865	Trp229	
32	-7.392	Tyr181	
33	-7.163	Tyr181, Tyr188	
36	-8.461	Trp229	
37	-8.711	Trp229	
38	-7.273	Tyr181	
41	-7.845	Trp229	
43	-6.631	Tyr181	
46	-7.915	Trp229	
47	-7.146	Trp229	
48	-8.002	Trp229	
49	-6.942	Trp229	
52	-7.784	Trp229	
53	-7.053	Tyr181	
57	-6.362	Tyr188	
58	-7.461	Trp229	Cl-Lys103
59	-6.584	Tyr188	
60	-5.427	Pro236	
61	-6.362	Tyr188	
77	-6.965	Tyr181	
78	-8.207	Trp229	
91	-7.605	Trp229	
93	-7.175	Trp229	
102	-7.124	Tyr188	
103	-5.788	Tyr181	
111	-7.379	Trp229	

Continued

115	-6.411	Pro236	
122	-6.569	Trp229	
123	-5.635	Pro236	
128	-9.083	Trp229	
132	-6.562	Tyr181	Cl-Lys103
133	-6.874	Trp229	
136	-6.509	Tyr181	Cl-Lys103
138	-8.164	Trp229	
143	-6.764	Pro236, Tyr188	
146	-6.970	Tyr188	
148	-8.160	Trp229	
158	-6.884	Tyr181	
167	-6.683	Tyr181	
171	-7.547	Trp229	
173	-5.778	Pro236	
183	-3.913	Pro236	
198	-6.562	Trp229	
202	-7.060	Pro236	
203	-6.023	Pro236	
208	-6.719	Trp229	
221	-7.194	Tyr188	
228	-6.645	Tyr188	
232	-6.878	Trp229	
243	-7.253	Tyr188	
255	-7.056	Tyr188	
258	-6.774	Trp229	Cl-Lys103
260	-6.999	Tyr188	
263	-7.325	Trp229	
266	-6.424	I-Pro236	
270	-6.988	I-Pro236	
288	-8.382	Trp229	
Average	-7.083		
Std. Dev.	-0.854		

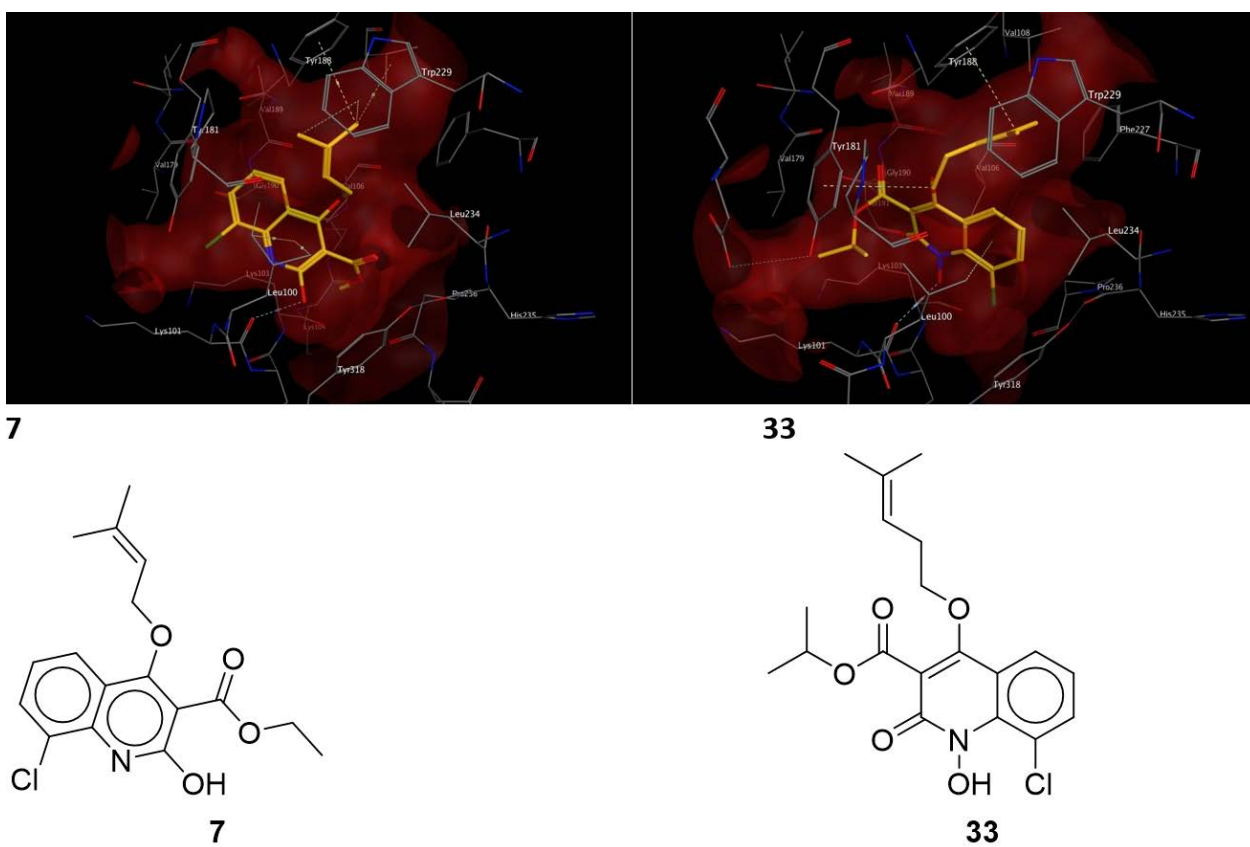


Figure 6. Binding modes of structures **7** and **123** with double interaction with aminoacids in RT PDB ID: 2B5J. There are contacts with Trp229 and Tyr188 for Structure **7**; and contacts Tyr181 and Tyr188 for structure **33**.

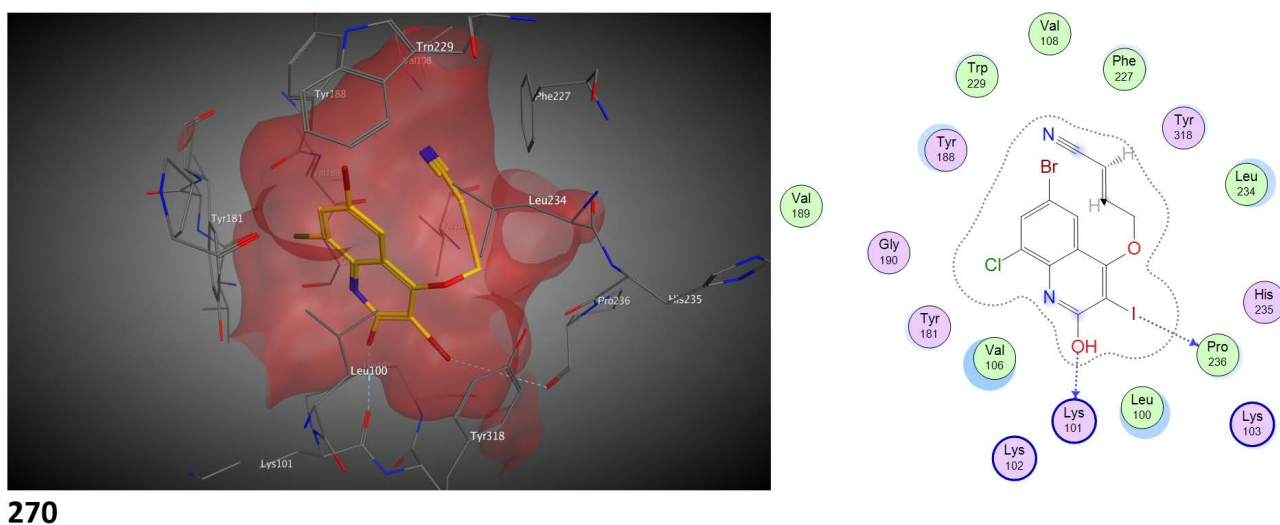


Figure 7. Docking model of structure **270** in the allosteric pocket of RT PDB ID: 2B5J showing an interaction of iodine in C-3 with Pro236.

the allosteric site and the flexibility of the substituent in C-4 let the ligand to make contact with Tyr181 or Trp229 (**Figure 8**). As example of this, we show docking of **58**.

Another interesting result was observed with the docking of **143** (**Figure 9**),

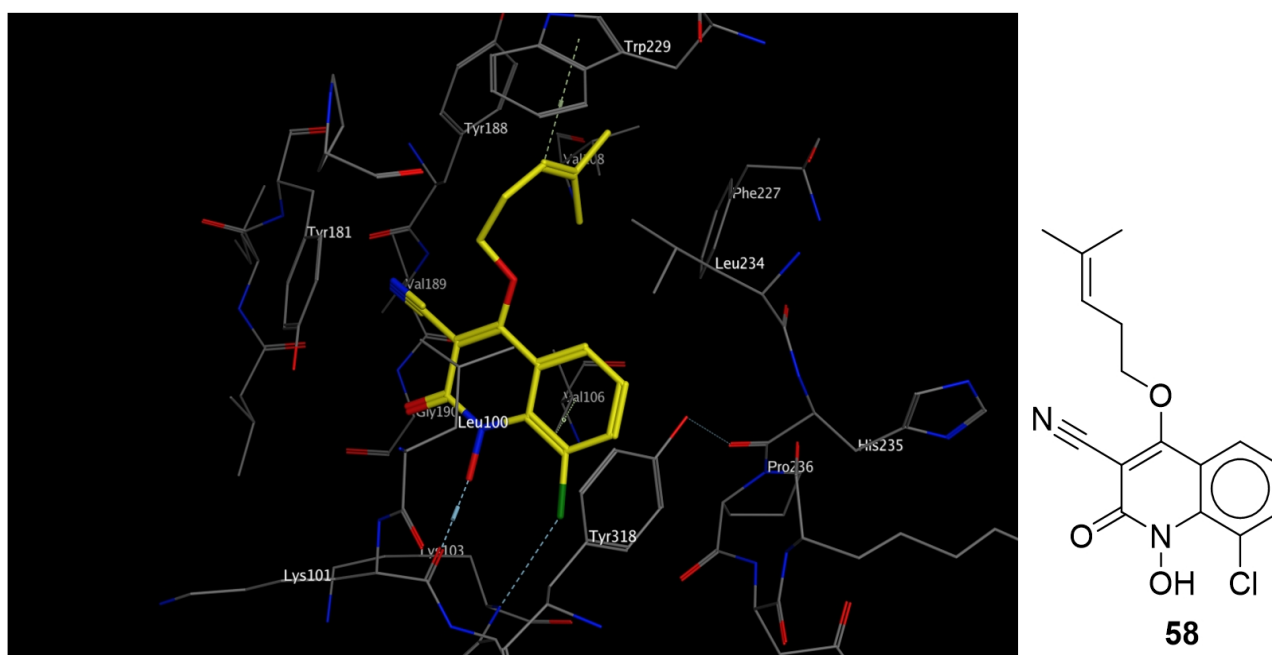


Figure 8. Binding mode of structure **58** in the allosteric pocket of RT PDB ID: 2B5J where is possible to observe interactions between hydrogen of NOH and Lys101; chlorine in C-8 with Lys103 and substituent in C-4 with Trp229.

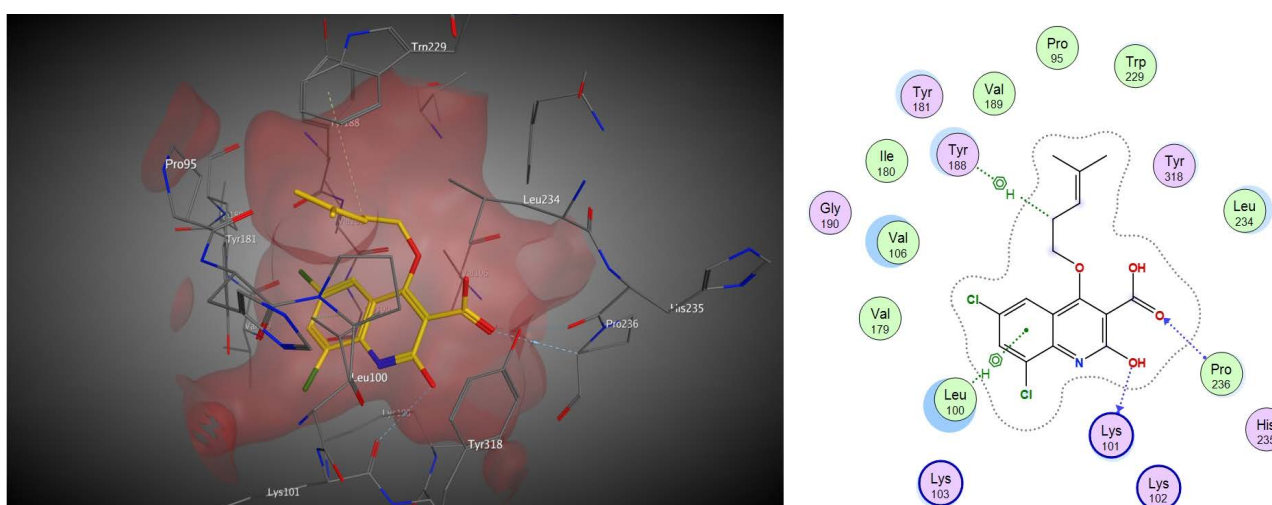


Figure 9. Docking model of structure **143** in the allosteric site of RT PDB ID: 2B5J showing interaction with aminoacids Lys101, Leu100, Pro236 and Tyr188.

which at same time show interaction with Tyr188 and pro236 with C-4 and C-3 substituents respectively. So, if the interaction with Tyr188 is lost because a mutation the compound could maintain activity against RT because Pro236, which is an aminoacid, conserved.

We found 21 structures that coincide in **Table 2** and **Table 3**; this could mean that they have a better probability to be RT inhibitors. Some structures have contact with conserved aminoacids, as Trp229 and Pro236 mentioned by Li *et al.* [5] which is favorable because this evidence give more probability to think that this contacts could help in the activity of the compounds. In the **Table 4** are

Table 4. Structures that are matching in **Table 2** and **Table 3**.

# OF STRUCTURE	INTERACTIONS: PDB ID: 2BAN	INTERACTIONS: PDB ID: 2B5J	Halogen in C-8 (interaction)
2	Trp229	Tyr188	
41	Trp229	Trp229	
47	Trp229	Trp229	
48	Trp229	Trp229	
58	Trp229	Tyr188	
91	Trp229	Tyr188	
102	Tyr188	Tyr188	
122	Trp229	Tyr188	
123	Pro236	Pro236, Trp229	Cl-Pro236
128	Trp229	Trp229	
133	Trp229	Trp229	
134	Tyr188	Pro236	Cl-Pro236
138	Trp229	Trp229	
146	Tyr188	Pro236	
148	Trp229	Tyr188	
158	Tyr181	Pro236, Trp229	
167	Tyr181	Tyr188	
192	Tyr188	Pro236	Cl-Pro236
202	Pro236	Pro236, Tyr188	Cl-Pro236
203	Pro236	Pro236	Cl-Pro236
228	Tyr188	Tyr188	

shown the 21 structures and the aminoacid of contact depending of PDB structure of RT.

3.6. Validation of the Docking Protocol with IN

In order to validate the docking with IN, we re-docked the co-crystal ligand in PDB ID: 3L2U (**Figure 10**), Elvitegravir. The binding mode was reproducible by MOE with a RMSD value of 1.3 Å (similar to our previous work [1]).

3.7. Docking with IN

We docked 73 selected quinolone structures that showed key interactions in the docking models with PDB ID: 2BAN and 2B5J, respectively. The docking with IN was done with the structure of IN PDB ID: 3L2U (Structures of quinolones in supplementary material as **Figure S1**). The quinolones have ester or carboxylic acid groups at C-3 and carbonyl group in C-2. Similar to the quinolones, Elvitegravir has a carboxylic acid at C-3 and a carbonyl group at C-4. In **Table 5** is

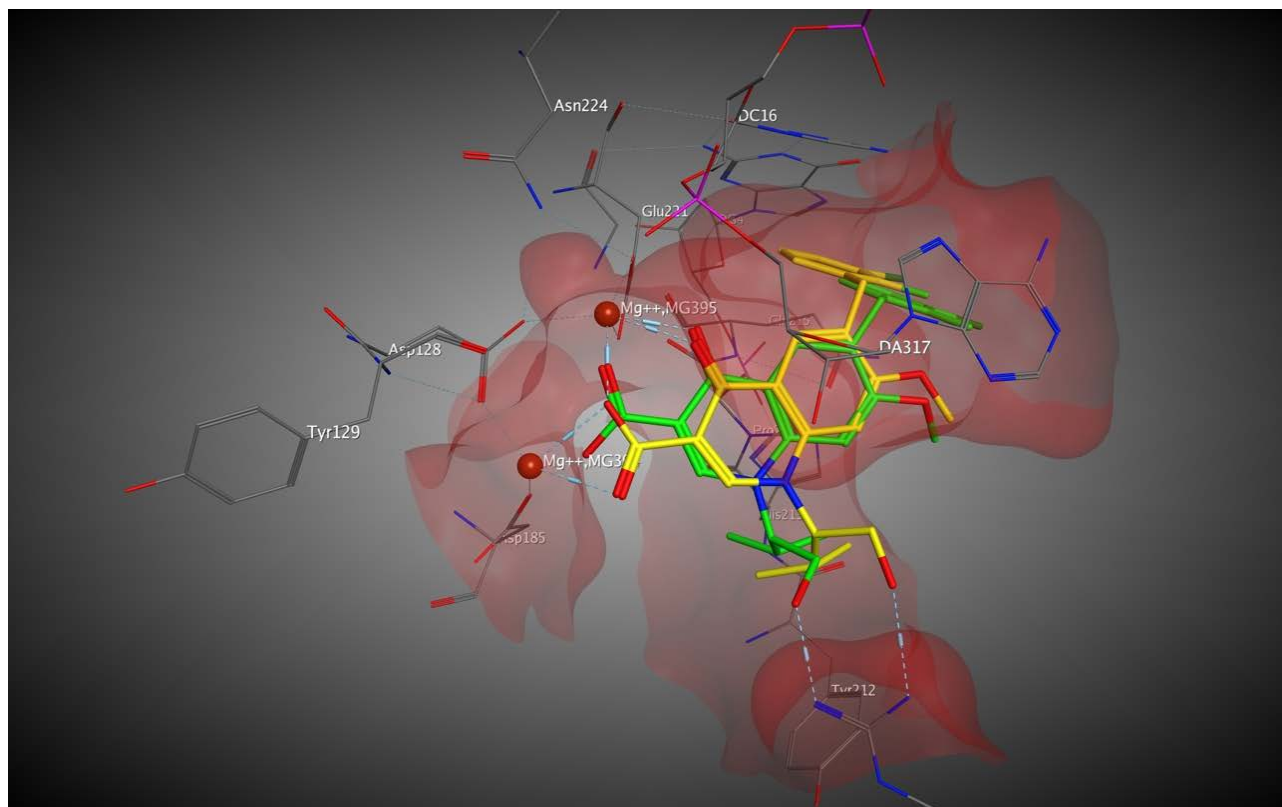


Figure 10. Re-docking of co-crystal (Elvitegravir) with the crystallographic structure of IN, PDB ID: 3L2U. The predicted binding pose is in green and the observed position in the crystallographic structure is in yellow. The RMSD value was 1.3 Å.

Table 5. Docking results with RT PDB ID: 3L2U.

ID	Score
42	-5.865
46	-6.503
47	-5.670
82	-4.031
83	-6.497
91	-5.970
102	-5.834
111	-6.609
138	-6.686
151	-6.387
152	-6.081
169	-5.104
213	-6.301
232	-6.044
Average	-5.999
Std. Dev.	0.686

summarized the results of 14 structures with potential to be dual inhibitors of RT and IN.

In **Table 5** we can see how quinolone **138** have the best result of score docking (-6.686) with PDB ID: 3L2U and have similar interaction to Elvitegravir with the two Mg^{++} ions (**Figure 11**). In the **Figure 11**, we can see in yellow color the quinolone overlapped on Elvitegravir (green color). The distances and the space IN-DNA between the Mg^{++} ions and the oxygens of quinolone has an average of 2.5 \AA according with MOE. The distances between Mg^{++} ions and Elvitegravir in MOE are near to 2 \AA .

The less favorable result in docking with 3L2U is for quinolone **82** because have a score of -4.031 . The distances between oxygens in quinolone and the Mg^{++} ions have an average of 2.6 \AA . The **Figure 12** show the interactions of quinolone and Mg^{++} in the space between IN and DNA.

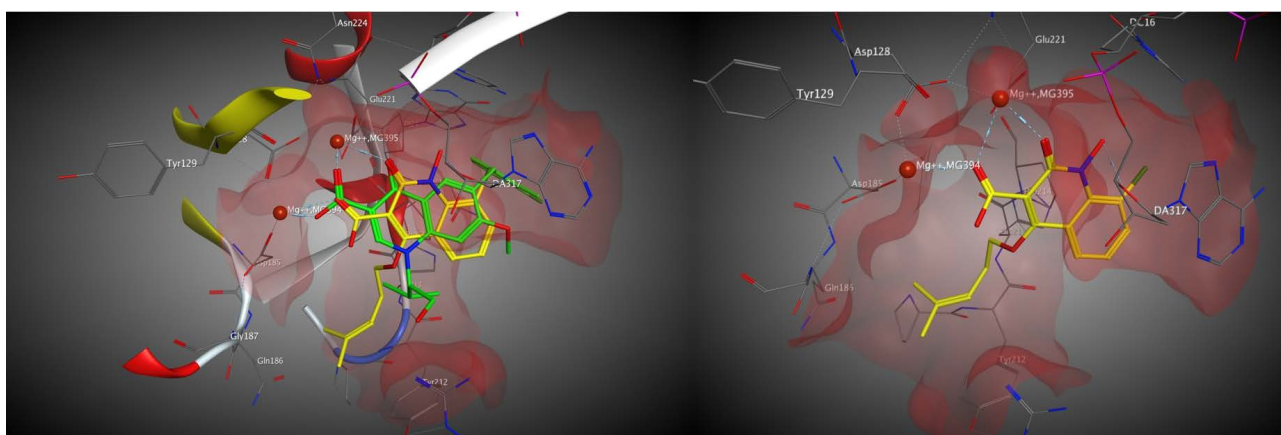


Figure 11. Docking of structure **138** showing interactions with Mg^{++} ions. In yellow quinolone **138** and in green Elvitegravir structure.

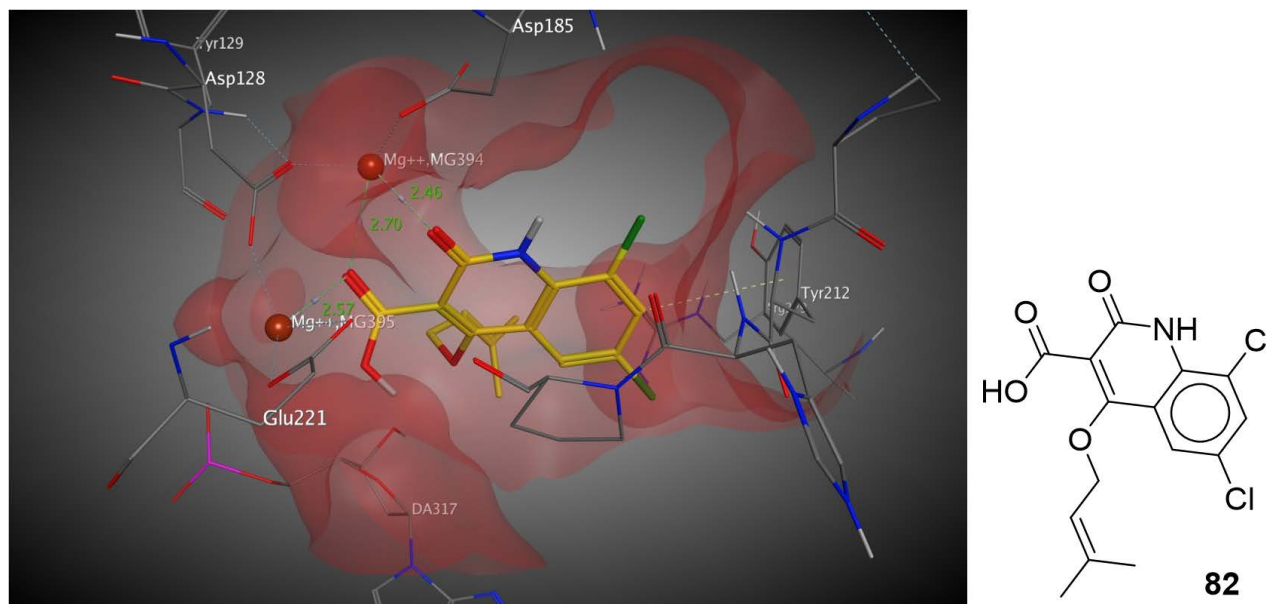


Figure 12. Docking of structure **82** showing interactions with Mg^{++} ions and distances between oxygen and Mg^{++} ions.

3.8. Quinolones Potential Dual Inhibitors of RT and IN

As result of the entire analysis of docking with RT and IN we got 14 quinolones that could act like dual inhibitors. In **Figure 13** is showing the five best structures that could be dual inhibitors. The first five structures are recommended to be synthesized according with the score results and the contact with Mg^{++} ions and aminoacids of interest in the space between IN-DNA and the allosteric space in RT, respectively.

3.9. Drug-Like Properties

The structures identified as potential compounds with activity against RT and IN were evaluated in base to the rules of Lipinski and Veber, which comprise six pharmacological properties of interest. The pharmacological properties calculated to 73 structures were MW, Log P, HBD and HBA, RB and TPSA. The results are included in supplementary material (**Table S2**).

4. Conclusions and Perspective

The results of docking with RT reveal in MOE that chlorine in C-8 of the quinolone could has the capacity to interact with Pro236 or Lys103 forming a halogen bond. The most important halogen interaction is with an oxygen atom of the carbonyl group of Pro236. Pro236 is a conserved aminoacid that could contribute to the inhibition activity of RT even help to preserve the activity with

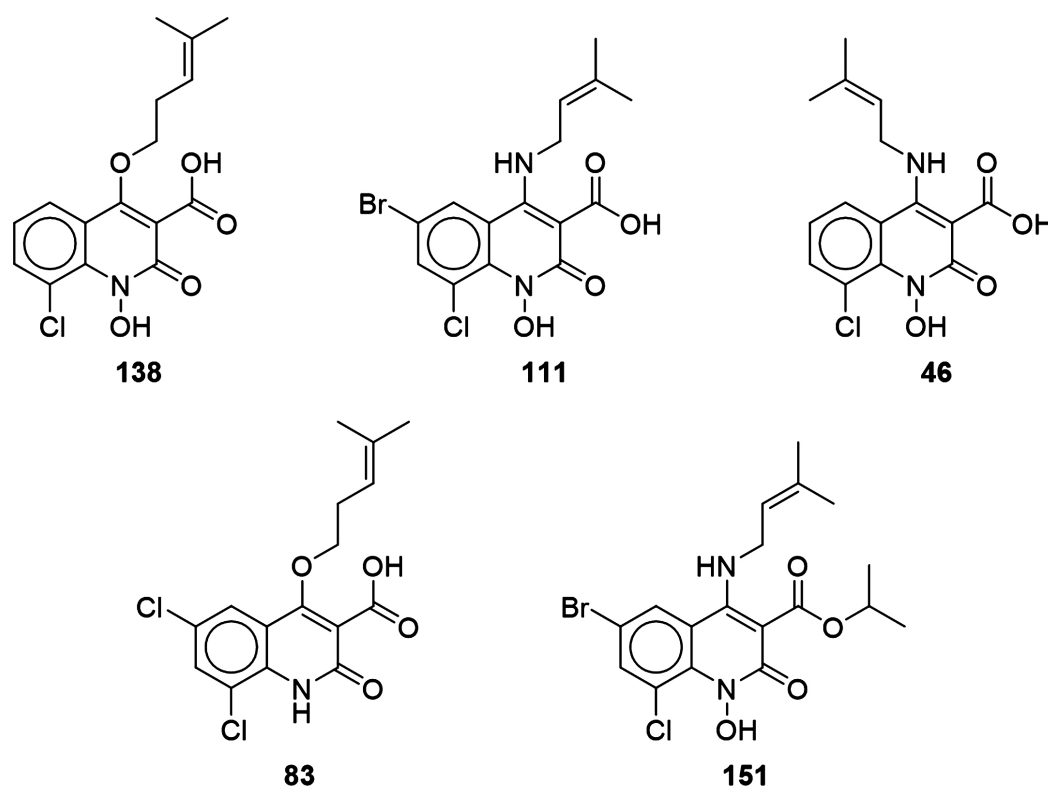


Figure 13. Chemical structures of the most promising quinoline-based compounds as potential dual inhibitors reverse transcriptase and integrase of HIV.

mutant strains of HIV. After analysis of the docking results of 320 quinolone structures with PDB ID: 2BAN, 2B5J and 3L2U, 14 structures were identified with possible dual activity in inhibition of RT and IN. There was not any halogen interaction between the 14 structures and IN. The most promising compounds to be synthesized are the quinolones **138**, **111**, **46**, **83** and **151** (Figure 13). The structure **151** shown halogen interaction with Pro236 in RT. The binding mode adopted by molecules **111**, **46** and **151** is like molecule **138** in Figure 11, while molecule **83** adopted a binding mode like quinolone **82** in Figure 12.

The main perspective of this work is synthesizing the structures proposed in this work and perform their biological evaluation (assays of cytotoxicity and inhibition of the activity of RT and IN) with the purpose of verifying the computational results.

Acknowledgements

A.C.V. is grateful to CONACyT and UNAM for the postdoctoral scholarship #291222. This work was supported by the Instituto de Investigaciones Biomédicas, UNAM through the program Nuevas Alternativas de Tratamiento para Enfermedades Infecciosas (Novel Alternatives for the Treatment of Infection Diseases) (NUATEI-IIB-UNAM), and Programa de Apoyo a la Investigación y el Posgrado (PAIP) grant 5000-9163, Facultad de Química, UNAM.

Conflicts of Interest

The authors declare no conflicts of interest regarding the publication of this paper.

References

- [1] Cabrera, A., Chávez, D., Huerta, L. and Medina-Franco, J.L. (2018) Molecular Modeling of Potential Dual Inhibitors of HIV Reverse Transcriptase and Integrase. *Computational Molecular Bioscience*, **8**, 1-41. <https://doi.org/10.4236/cmb.2018.81001>
- [2] Cabrera, A., Chávez, D., Reyes, H., *et al.* (2015) Crystal Structure of Ethyl 2,4-Dichloroquinoline-3-Carboxylate. *Acta Crystallographica*, **E71**, o939.
- [3] Hopkins, A.L., Ren, J., Milton, J., *et al.* (2004) Design of Non-Nucleoside Inhibitors of HIV-1 Reverse Transcriptase with Improved Drug Resistance Properties. 1. *Journal of Medicinal Chemistry*, **47**, 5912-5922. <https://doi.org/10.1021/jm040071z>
- [4] Medina-Franco, J.L., Martínez-Mayorga, K., Juárez-Gordiano, C. and Castillo, R. (2007) Pyridin-2(1H)-Ones: A Promising Class of HIV-1 Non-Nucleoside Reverse Transcriptase Inhibitors. *ChemMedChem*, **2**, 1141-1147. <https://doi.org/10.1002/cmdc.200700054>
- [5] Li, A., Ouyang, Y., Wang, Z., *et al.* (2013) Novel Pyridinone Derivatives as Non-Nucleoside Reverse Transcriptase Inhibitors (NNRTIs) with High Potency against NNRTI-Resistant HIV-1 Strains. *Journal of Medicinal Chemistry*, **56**, 3593-3608. <https://doi.org/10.1021/jm400102x>
- [6] Tang, J., Maddali, K., Dreis, C.D., *et al.* (2011) N-3 Hydroxylation of Pyrimidine-2,4-Diones Yields Dual Inhibitors of HIV Reverse Transcriptase and Integrase.

- ACS Medicinal Chemistry Letters*, **2**, 63-67. <https://doi.org/10.1021/ml1002162>
- [7] Freeman, G.A., Andrews III, C.W., Hopkins, A.L., et al. (2004) Design of Non-Nucleoside Inhibitors of HIV-1 Reverse Transcriptase with Improved Drug Resistance Properties. 2. *Journal of Medicinal Chemistry*, **47**, 5923-5936. <https://doi.org/10.1021/jm040072r>
- [8] Tang, J., Maddali, K., Pommier, Y., Sham, Y.Y. and Wang, Z. (2010) Scaffold Rearrangement of Dihydropyrimidine Inhibitors of HIV Integrase: Docking Model Revisited. *Bioorganic and Medicinal Chemistry Letters*, **20**, 3275-3279. <https://doi.org/10.1016/j.bmcl.2010.04.048>
- [9] Politzer, P., Murray, J.S. and Clark, T. (2010) Halogen Bonding: An Electrostatically-Driven Highly Directional Noncovalent Interaction. *Physical Chemistry Chemical Physics*, **12**, 7748-7757. <https://doi.org/10.1039/c004189k>
- [10] AIDSinfo (2018) Understanding HIV/AIDS. Fact Sheets. FDA-Approved HIV Medicines. <https://aidsinfo.nih.gov/understanding-hiv-aids/fact-sheets/21/58/fda-approved-hiv-medicines>
- [11] AIDSinfo (2018) Drugs. Doravirine. <https://aidsinfo.nih.gov/drugs/546/doravirine/0/professional>
- [12] Mendez-Lucio, O., Naveja, J.J., Vite-Caritino, H., Prieto-Martinez, F.D. and Medina-Franco, J.L. (2013) One Drug for Multiple Targets: A Computational Perspective. *Journal of the Mexican Chemical Society*, **60**, 168-181.
- [13] Himmel, D.M., Das, K., Clark, A.D., et al. (2005) Crystal Structures for HIV-1 Reverse Transcriptase in Complexes with Three Pyridinone Derivatives: A New Class of Non-Nucleoside Inhibitors Effective against a Broad Range of Drug-Resistant Strains. *Journal of Medicinal Chemistry*, **48**, 7582-7591. <https://doi.org/10.1021/jm0500323>
- [14] Berman, H.M., Westbrook, J., Feng, Z., et al. (2000) The Protein Data Bank. *Nucleic Acids Research*, **28**, 235-242. <https://doi.org/10.1093/nar/28.1.235>
- [15] Hare, S., Gupta, S.S., Valkov, E., Engelman, A. and Cherepanov, P. (2010) Retroviral Intasome Assembly and Inhibition of DNA Strand Transfer. *Nature*, **464**, 232-236. <https://doi.org/10.1038/nature08784>
- [16] Molecular Operating Environment (MOE) (2014) Chemical Computing Group Inc., Montreal. <https://www.chemcomp.com/>
- [17] Krusemark, C.J. (2012) Drug Design: Structure- and Ligand-Based Approaches. *The Quarterly Review of Biology*, **87**, 165.
- [18] Kerns, E.H. and Di, L. (2016) Drug-Like Properties: Concepts, Structure Design and Methods: From ADME to Toxicity Optimization. Academic Press, Amsterdam, 31.
- [19] Radi, M., Falciani, C., Contemori, L., et al. (2008) A Multidisciplinary Approach for the Identification of Novel HIV-1 Non-Nucleoside Reverse Transcriptase Inhibitors: S-DABOCs and DAVPs. *ChemMedChem*, **3**, 573-593. <https://doi.org/10.1002/cmdc.200700198>
- [20] Medina-Franco, J.L., Rodríguez-Morales, S., Juárez-Gordiano, C., Hernández Campos, A., Jiménez-Barbero, J. and Castillo, R. (2004) Flexible Docking of Pyridinone Derivatives into the Non-Nucleoside Inhibitor Binding Site of HIV-1 Reverse Transcriptase. *Bioorganic and Medicinal Chemistry*, **12**, 6085-6095. <https://doi.org/10.1016/j.bmc.2004.09.008>
- [21] Medina-Franco, J.L., Rodríguez-Morales, S., Juárez-Gordiano, C., Hernández Campos, A. and Castillo, R. (2004) Docking-Based CoMFA And CoMSIA Studies of

Non-Nucleoside Reverse Transcriptase Inhibitors of the Pyridinone Derivative Type. *Journal of Computer Aided Molecular Design*, **18**, 345-360.
<https://doi.org/10.1023/B:JCAM.0000047816.15514.ab>

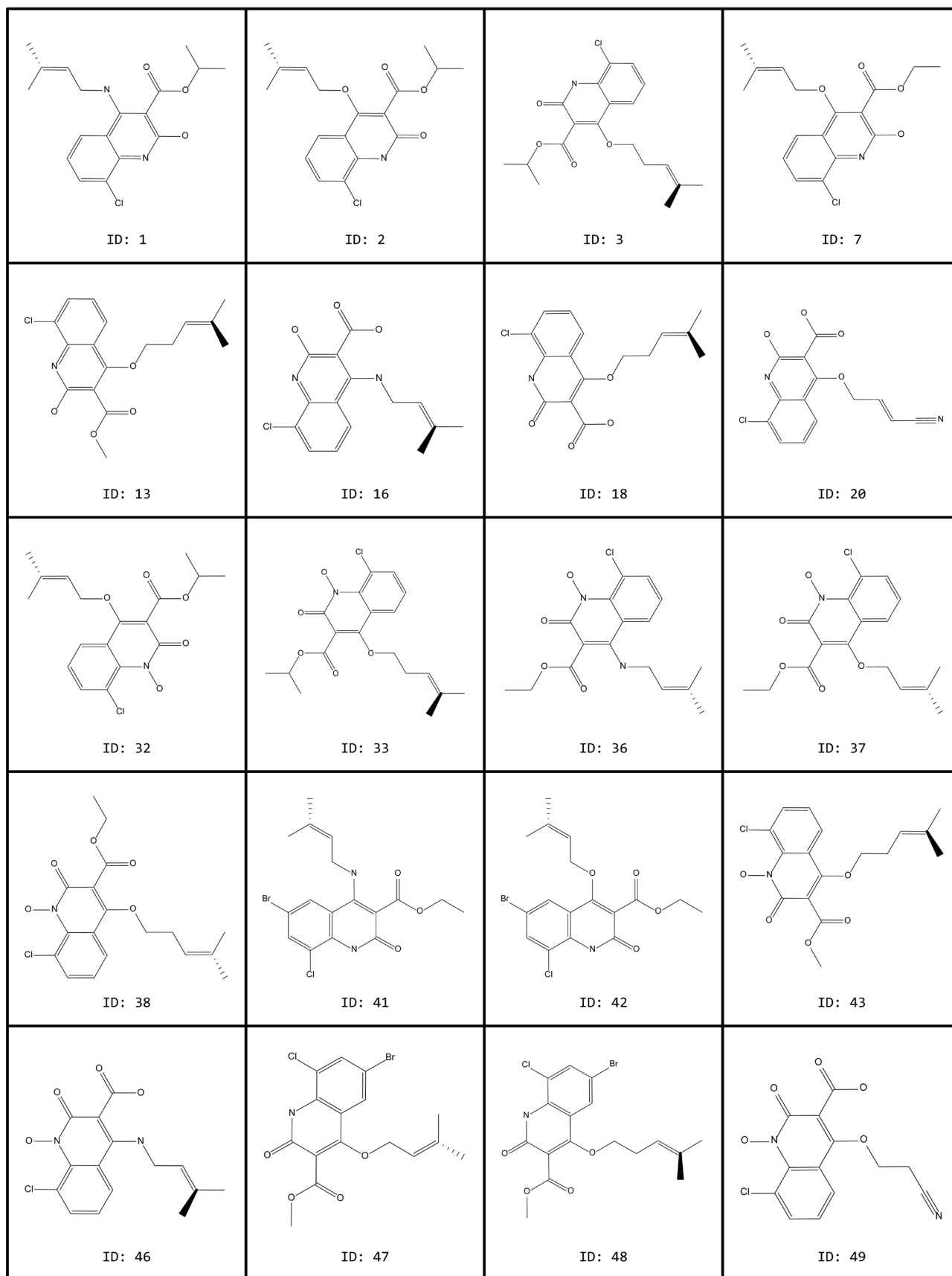
Supplementary Material

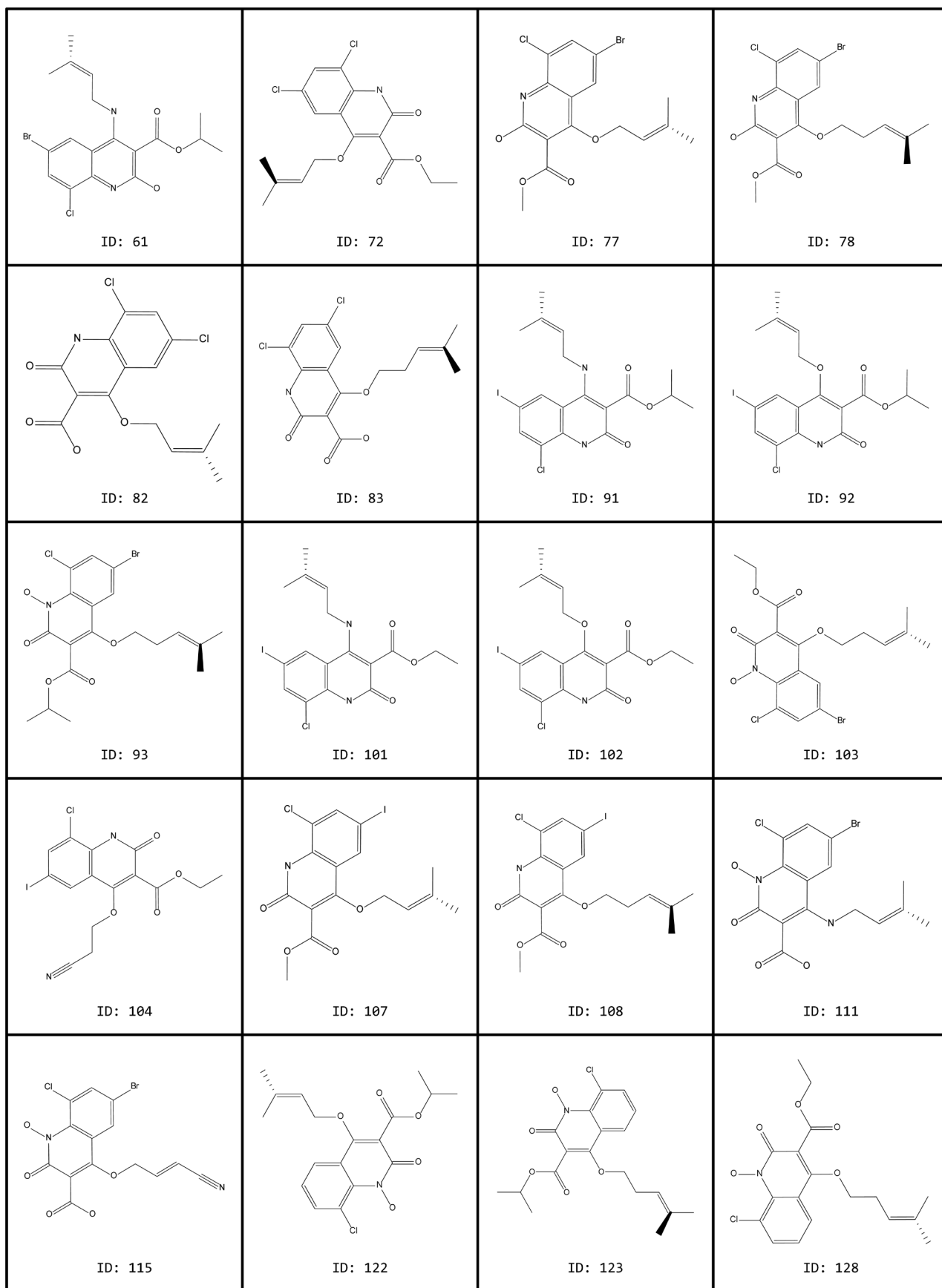
Table S1. 3D alignment scores (kcal/mol) calculated with MOE of 32 selected compound with the structure of two co-crystallized pyridinones.

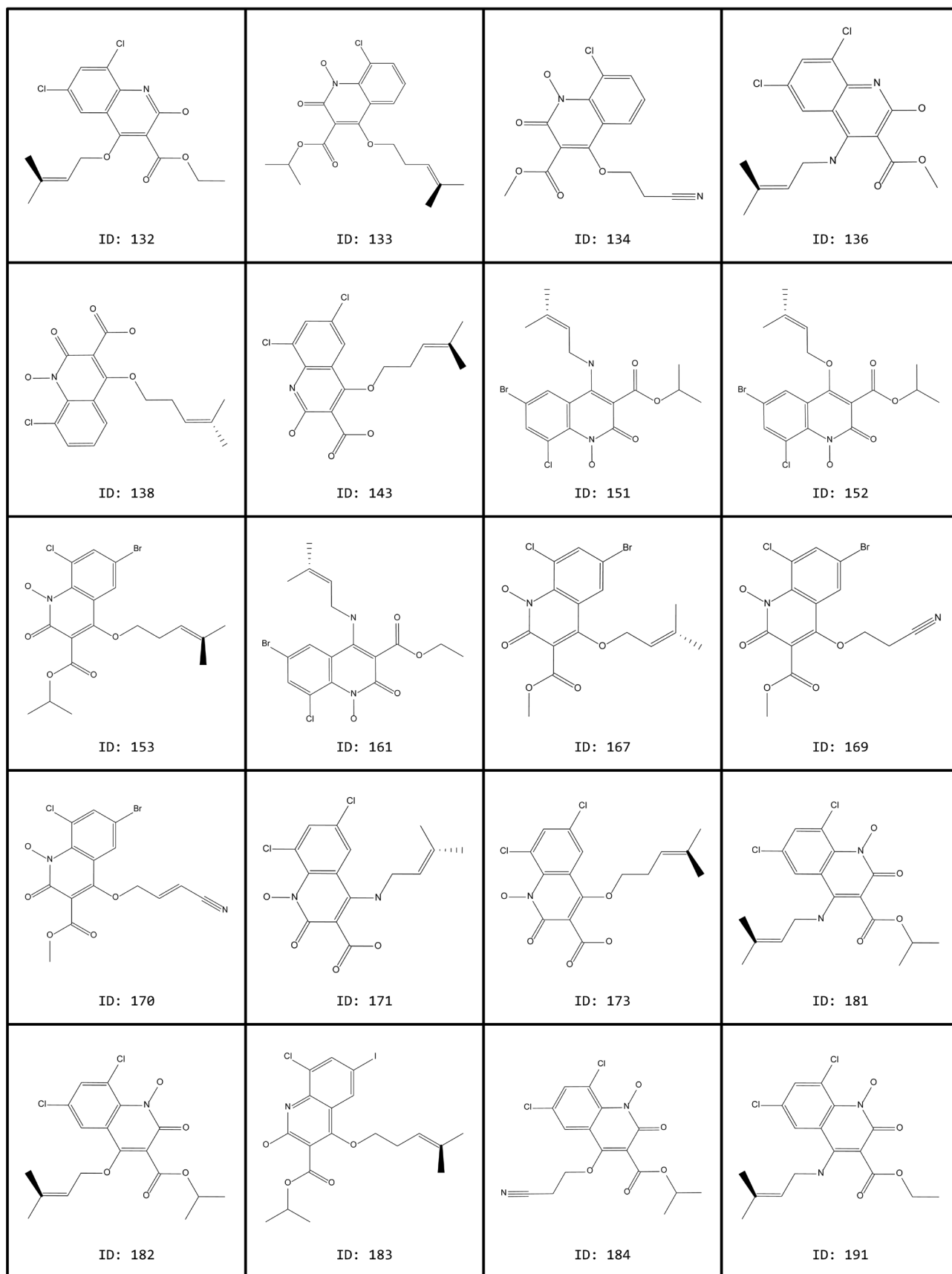
ID	R157208	R165481
10	-72.1146	-83.9869
20	-86.0508	-81.9987
30	-77.5192	-84.8052
40	-85.4631	-92.0709
50	-74.1501	-96.4579
60	-86.5782	-88.9039
70	-83.6632	-93.2938
80	-93.4436	-74.8226
90	-70.14	-97.9708
100	-76.3413	-80.4863
110	-103.698	-93.2389
120	-76.968	-89.1745
130	-77.801	-81.0855
140	-64.038	-100.687
150	-90.5816	-77.0796
160	-85.6552	-87.0859
170	-104.058	-92.3016
180	-79.5108	-83.4159
190	-84.9452	-72.8596
200	-75.2163	-85.3578
210	-83.6687	-86.5658
220	-82.4579	-82.4668
230	-65.9072	-91.0722
240	-80.5505	-77.274
250	-75.0684	-72.0681
260	-66.0169	-63.9789
270	-79.3474	-83.7659
280	-78.3733	-62.4943
290	-69.3394	-99.2574
300	-86.3217	-91.1956
310	-68.563	-53.3706
320	-78.0818	-68.356
Average	-80.051	-83.4046
Std. Dev.	9.583484	11.1369

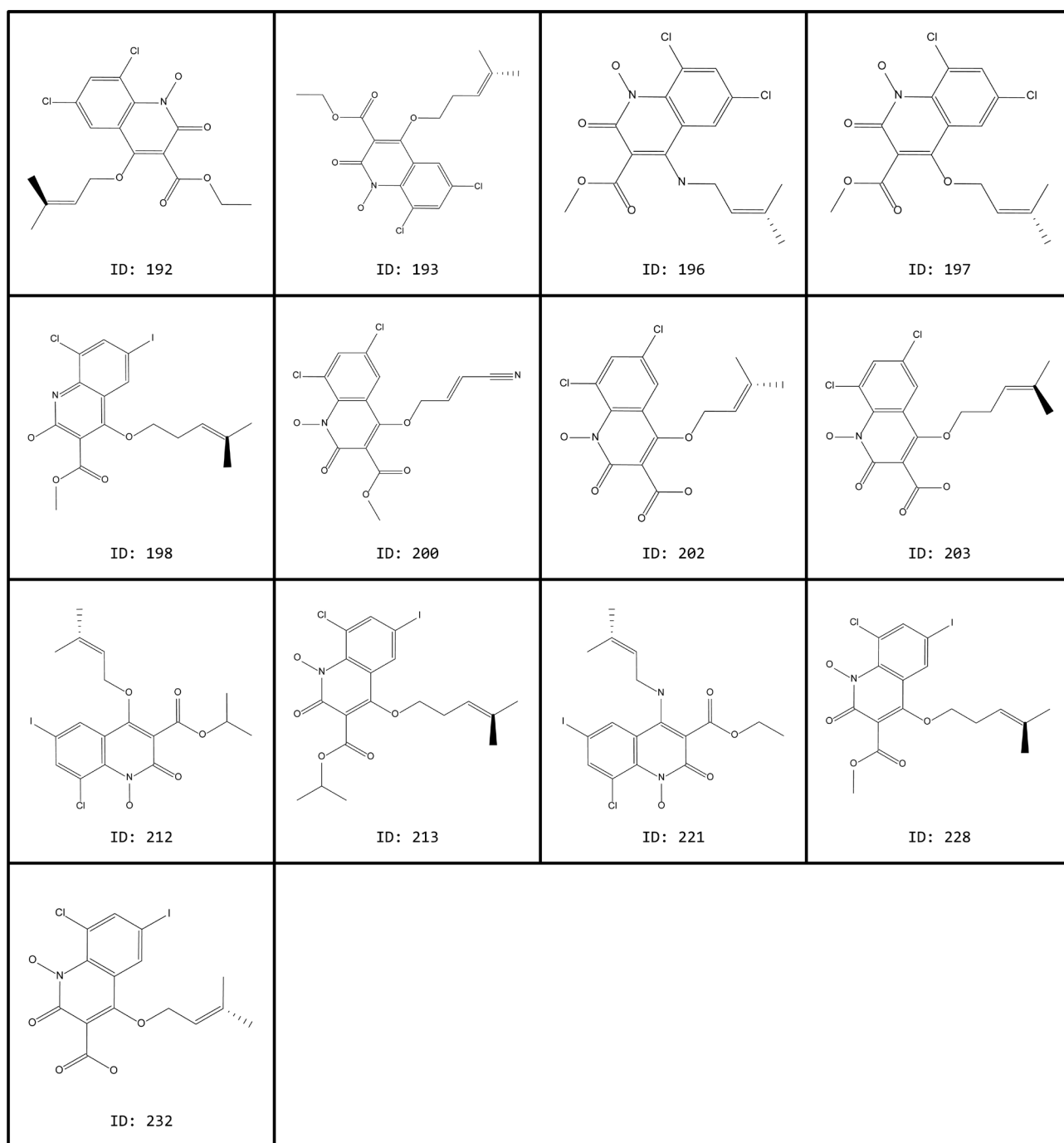
Table S2. Drug-like properties of newly designed compounds as potentially inhibitors of RT an IN.

# of Structure	MW	log P	HBD	HBA	RB	TPSA	# of Structure	MW	log P	HBD	HBA	RB	TPSA
1	348.83	4.5	2	3	6	71.4	122	365.81	3.7	1	4	6	76.1
2	349.81	3.9	1	3	6	64.6	123	379.84	4.1	1	4	7	76.1
3	363.84	4.3	1	3	7	64.6	128	365.81	3.7	1	4	7	76.1
7	335.79	4.1	1	4	6	68.7	132	370.23	4.8	1	4	6	68.7
13	335.79	4.1	1	4	6	68.7	133	379.84	4.1	1	4	7	76.1
16	306.75	3.7	4	4	4	82.4	134	322.7	1.9	1	5	6	99.9
18	321.76	3.5	3	4	5	75.6	136	355.22	4.4	2	3	5	71.4
20	304.69	2.8	3	6	5	103.4	138	337.76	3.2	3	5	5	87.1
32	365.81	3.7	1	4	6	76.1	143	356.2	4.7	3	5	5	79.7
33	379.84	4.1	1	4	7	76.1	151	443.73	4.1	2	3	6	78.9
36	350.8	2.9	2	3	6	78.9	152	444.71	4.5	1	4	6	76.1
37	351.79	3.3	1	4	6	76.1	153	458.74	4.9	1	4	7	76.1
38	365.81	3.7	1	4	7	76.1	161	429.7	3.7	2	3	6	78.9
41	413.7	3.9	2	2	6	67.4	167	416.66	3.7	1	4	5	76.1
42	414.68	4.3	1	3	6	64.6	169	401.6	2.7	1	5	6	99.9
43	351.79	3.3	1	4	6	76.1	170	413.61	2.8	1	5	6	99.9
46	322.75	2.4	4	4	4	89.9	171	357.19	3.1	4	4	4	89.9
47	400.66	3.9	1	3	5	64.6	173	372.2	3.9	3	5	5	87.1
48	414.68	4.3	1	3	6	64.6	181	399.27	3.9	2	3	6	78.9
49	308.68	1.8	3	6	5	110.9	182	400.26	4.4	1	4	6	76.1
61	427.73	5.3	2	3	6	71.4	183	489.74	5.5	1	4	7	68.7
72	370.23	4.2	1	3	6	64.6	184	385.2	3.3	1	5	7	99.9
77	400.66	4.5	1	4	5	68.7	191	385.25	3.6	2	3	6	78.9
78	414.68	4.9	1	4	6	68.7	192	386.23	4	1	4	6	76.1
82	342.18	3.7	3	4	4	75.6	193	400.26	4.4	1	4	7	76.1
83	356.2	4.1	3	4	5	75.6	196	371.22	3.2	2	3	5	78.9
91	474.73	4.1	2	2	6	67.4	197	372.2	3.6	1	4	5	76.1
92	475.71	4.5	1	3	6	64.6	198	461.68	4.7	1	4	6	68.7
93	458.74	4.9	1	4	7	76.1	200	369.16	2.7	1	5	6	99.9
101	460.7	3.7	2	2	6	67.4	202	358.18	3.5	3	5	4	87.1
102	461.68	4.2	1	3	6	64.6	203	372.2	3.9	3	5	5	87.1
103	444.71	4.5	1	4	7	76.1	212	491.71	4.3	1	4	6	76.1
104	446.63	3.1	1	4	7	88.4	213	505.74	4.7	1	4	7	76.1
107	447.66	3.8	1	3	5	64.6	221	476.7	3.5	2	3	6	78.9
108	461.68	4.2	1	3	6	64.6	228	477.68	3.9	1	4	6	76.1
111	401.64	3.2	4	4	4	89.9	232	449.63	3.5	3	5	4	87.1
115	399.58	2.7	3	6	5	110.9							
Specification	<500	<5	<5	<10	<10	<140	Specification	<500	<5	<5	<10	<10	<140







**Figure S1.** 73 structures docked with RT.